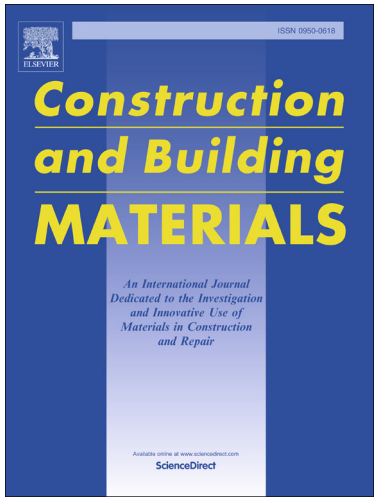

Interfacial Fracture Toughness of Composite Concrete Beams

Yougui Lin, John N. Karadelis

PII: S0950-0618(19)30908-0
DOI: https://doi.org/10.1016/j.conbuildmat.2019.04.066
Reference: JCBM 15639

To appear in: *Construction and Building Materials*

Received Date: 21 July 2018
Revised Date: 2 April 2019
Accepted Date: 8 April 2019

Please cite this article as: Y. Lin, J.N. Karadelis, Interfacial Fracture Toughness of Composite Concrete Beams, *Construction and Building Materials* (2019), doi: https://doi.org/10.1016/j.conbuildmat.2019.04.066

Interfacial Fracture Toughness of Composite Concrete Beams

Yougui Lin[1], John N. Karadelis[2]*

1. Guangxi Transport Technology Co. Ltd., Kunlun Ave., Nanning, Guangxi Province, P.R. China, 530028.
2. Faculty of Engineering Environment and Computing, Coventry University, W Midlands, CV1 5FB, UK.

Abstract:
A test for measuring the interfacial fracture toughness of a bi-material interface, essentially for concrete overlaid pavements was developed. The measured interfacial fracture toughness of steel fibre-reinforced, roller-compacted, polymer modified concrete (SFR-RC-PMC) onto ordinary Portland cement concrete (OPCC) was found to be 52.0 J/m^2 and 22.6 J/m^2 for rough and smooth interfaces respectively. The experimental interfacial fracture toughness results can be suitable for the design of overlays on worn concrete pavements. In addition, the measured interfacial fracture toughness was used to predict the cracking trajectory of the composite beams under four-point bending (4PB) tests. It was concluded that a single interfacial fracture parameter, the ERR (energy release rate) at interface, is an appropriate and sufficient parameter to assess the interfacial delamination performance of a composite beam under 4PB flexure.

Keywords: interface fracture; finite element analysis; delamination; concrete; toughness; stress-intensity-factors; energy-release-rate.

1. Introduction

A vast number of concrete structures, in particular concrete pavements, are in need of rehabilitation and strengthening around the world every year. Concrete overlays bonded on old concrete pavements to improve their structural capacity and safety are increasingly gaining acceptance in USA [1,2,3]. If the overlay is fully bonded with the existing concrete pavement leading to a thicker composite section, the result is a much stiffer pavement and a considerable decrease in vehicular load stresses. The key to success is to ensure that the two structures – the overlay and the existing pavement -respond as one under the action of thermal and vehicular loads [3].

Interfacial delamination results in the reduction of load bearing capacity, consequently leading to poor durability and compromise of safety. It is important to assess accurately the interfacial bond quality, and therefore to evaluate correctly the interfacial fracture parameters. As stress distribution in the crack line at the vicinity of the crack tip varies greatly due to *stress*

* Corresponding author: john.karadelis@coventry.ac.uk

singularity and "*oscillation*" at the crack tip, the strength-based criterion method for assessing delamination at interface is no longer the appropriate approach. Thus, it may be obligatory to employ interface fracture mechanics.

For most cases, a numerical method, such as the finite element analysis (FEA) and/or the boundary element analysis (BEA), are needed to extract fracture parameters for interfacial cracks due to the lack of analytical solutions. The three methods, i.e. the J-integral method [4,5, 6], the cracked faces displacement-based method [7, 8, 9] and the nodal force-based method [10,11,12,13], have been employed regularly to calculate interfacial fracture parameters. The J-integral method calculates the ERR (energy release rate: *energy dissipated during fracture, per unit of newly created fracture surface area*), by performing a contour integration [4, 5, 6], which is usually computed within the selected FE code. Rybicki and Kanninen [13] proposed a nodal force-based method for calculating SIFs (stress intensity factors) of homogeneous materials based on Irwin's crack closure integral [14]. Sridharan [15] used the nodal force and displacement technique and the mode separation method to evaluate the ERR, employing a complex calculation procedure. Bjerkén and Persson [10] employed the FE code ABAQUS, the decoupling concept and the nodal forces technique to calculate the SIFs. Xie and Biggers Jr. [12] developed a special interface element and embedded it in ABAQUS to compute ERR using the nodal force technique. All these methods had something in common. They appeared to be complicated, not convenient for practicing engineers. Thus, a simple but rigorous enough method for determining the ERR is desired for engineering applications.

Interfacial fracture mechanics have been employed since the 1990's to evaluate the interfacial fracture toughness. Charalambides et al. [16] provided the analytical solution for determining the interfacial ERR for the symmetrical test specimen shown in Figure 1(a), and then utilised the experimental set-up to test the interfacial resistance of a system consisting of polymethyl methacrylate bonded to aluminium. Later, Klingbeil and Beuth [17], and Huang et al. [18], employed the experimental of Figure 1(a) to measure the interfacial toughness of two metal

layers under four-point bend (4PB). Watanabe [19] investigated the interfacial delamination of mortar and ceramic tiles under shear loading. Wang and Suo [20], and Shi et al. [21] tested the interfacial toughness of adhesive joints using Brazil-nut-sandwich specimens; Büyüköztürk and Lee [22] studied the interfacial fracture toughness of a mortar-granite interface. Tschegg et al. [23] measured the interfacial fracture energy of concrete-to-concrete using the experimental approach shown in Figure 1(b). Satoh et al. [24] carried out several experiments (including the one shown in Figure 1(b)), employing tension softening diagrams to investigate the major factors affecting the crack path and measure the interfacial fracture toughness in a concrete-to-concrete interface setting. Chabot et al. [25,26] investigated the interfacial fracture behaviour of cement concrete and asphalt concrete. They used the arrangement illustrated in Figure 1(c), to investigate both the interfacial performance of cement concrete overlay on old asphalt pavements, and the water effect on the interfacial cracking behaviour.

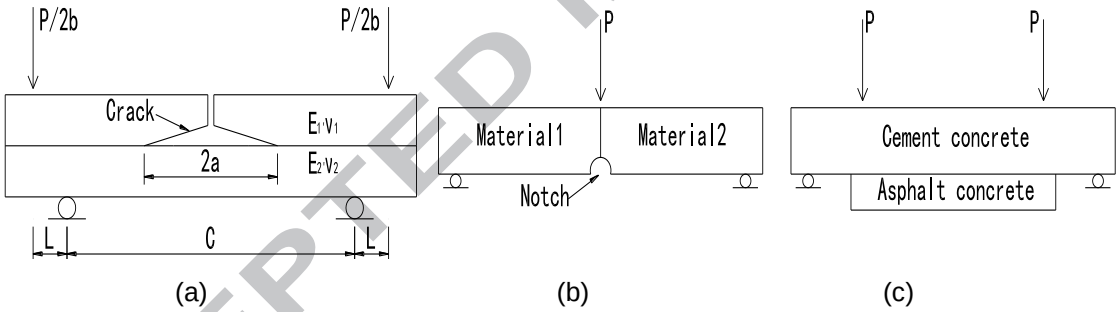

Figure 1. (a): bi-material beam with symmetrical interfacial cracks under 4PB; (b): bi-material beam with vertical interface under 3PB; (c): bi-material beam with horizontal interface under 4PB.

However, for concrete composite beams, the experimental setup demonstrated in Figure 1 (a) & (c) may not be appropriate, because the crack's trajectory may not develop on the axis of symmetry of the crack. Also, the arrangement shown in Figure 1(b) is not suitable for RCC (Roller Compacted Concrete) because the interface of overlay and old concrete pavement is always horizontal. After all, construction of a vertical interface cannot be possible due to dry mix [27,28,29].

Thus, an appropriate test specimen and loading configuration are essential for testing the interfacial fracture toughness of the concrete overlay on worn pavements. Indeed, this can be extended to study the interfacial fracture toughness of concrete–onto–concrete in general and assist with the design of concrete overlays on worn concrete pavements, in particular. Based on the above, a simple way for calculating the strain Energy Release Rate (ERR) of a bi-material interface using the method proposed in this article and the aid of a general finite element code, such as ANSYS [30], can be significant. Hence, a test specimen and loading configuration were setup and used to measure the interfacial fracture toughness for concrete overlay pavements.

This paper employs the theory of elasticity to calculate the ERR at the bi-material interface. It continues by measuring the interfacial fracture toughness of SFR.RC.PMC-to-OPCC (steel fibre reinforced, roller-compacted, polymer modified concrete–to–ordinary Portland cement concrete), under 3PB tests. Finally, it closes by predicting the crack's trajectory in a composite beam under 4PB based on both, the measured interfacial fracture toughness, and the ERR calculation approach.

2. Strain Energy Release Rate of Bi-Material Interface

Irwin's hypothesis [14] states that if a crack extends by a small amount, Δa, the energy absorbed in the process is equal to the work required to close the crack to its original length. However, accurate results cannot be obtained using the stress along the crack line, due to the large variation of stresses along the interface, encouraged by conditions like *stress singularity* (stresses reaching infinite values) and *stress oscillation* at the crack tip. Therefore, the nodal force-based method proposed by Rybicki and Kanninen [13] may be a good start.

The above method has been addressed briefly by the authors in reference [31]. A calculation procedure for obtaining the ERR using nodal force and relative nodal displacement techniques with the aid of FE code ANSYS [30], is presented in detail below, aiming

primarily for practicing engineers. Figure 2(a) represents the original model meshed by square elements with identical length, L_0, surrounding the crack tip. Figure 2(b) shows the crack extension by a small amount Δa, (Δa= L_0). Plane strain conditions are assumed.

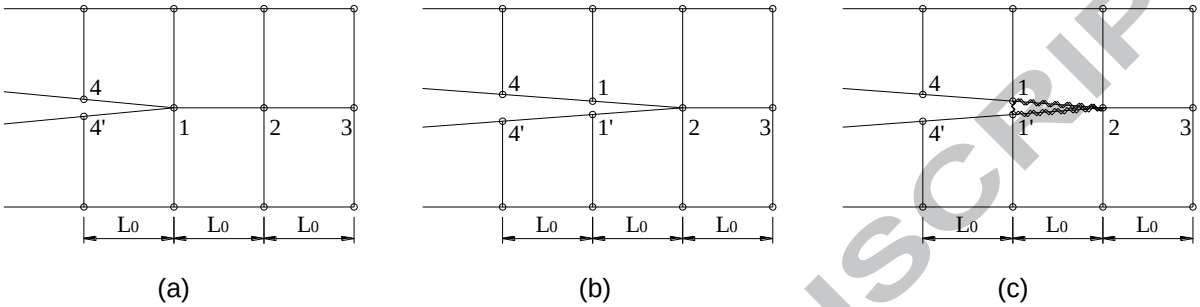

Figure 2. (a): Original meshed Model-a. Area around crack tip is meshed with square elements of equal size; (b): Meshed Model-b. Crack extends by $\Delta a = L_0$. (c): Meshed Model-c: Three springs with very high stiffness are now introduced.

The relative opening and sliding displacements of nodes 1 and $1'$ obtained by analysing the loaded Model-b, can be calculated using the relationships below:

$$\delta_{1x} = \left| u_{1x}^{(a)} - u_{1x}^{(b)} \right| \quad (1)$$

$$\delta_{1y} = \left| u_{1y}^{(a)} - u_{1y}^{(b)} \right| \quad (2)$$

$$\delta_{1'x} = \left| u_{1x}^{(a)} - u_{1'x}^{(b)} \right| \quad (3)$$

$$\delta_{1'y} = \left| u_{1y}^{(a)} - u_{1'y}^{(b)} \right| \quad (4)$$

Referring to Figure 2: $u_{1x}^{(a)}, u_{1y}^{(a)}$ are displacements of node 1, of the loaded Model-a; $u_{1x}^{(b)}$, $u_{1y}^{(b)}, u_{1'x}^{(b)}$, $u_{1'y}^{(b)}$ are displacements of loaded Model-b for nodes 1 and $1'$, respectively. Numerical analysis of loaded Model-c, in Figure2(c), can provide the nodal forces: F_{1x},F_{1y}, $F_{1'x}$ and $F_{1'y}$. It is noted that: $F_{1y} = F_{1'y}$. The equations for calculating the ERRs are presented by the authors in reference [31].

3. Test Rig and Load Configuration. Engineering Practice.

The specimen and loading configuration for testing interfacial toughness for concrete overlays bonded on worn concrete pavements should replicate closely the mechanical behaviour of the real system. Figure 3(a) represents the real situation in a diagrammatic mode as the inherent interfacial crack will open under vehicular loading. This has been studied earlier by the authors [31]. The loading configuration proposed in Figure 3(b) is a reasonable test setup for simulating the pavement system, as it forces the crack to propagate along the interface and minimises the probability of it to reflect upwards. Hence, it was adopted to study and measure the interfacial fracture toughness. It is pointed out that the experimental set-up in Figure 3(b), named *single-leg composite beam*, was used with monotonic loading and fatigue tests to investigate the critical ERR and fatigue life of polymer-metal interface by Poshtan et al.[32].

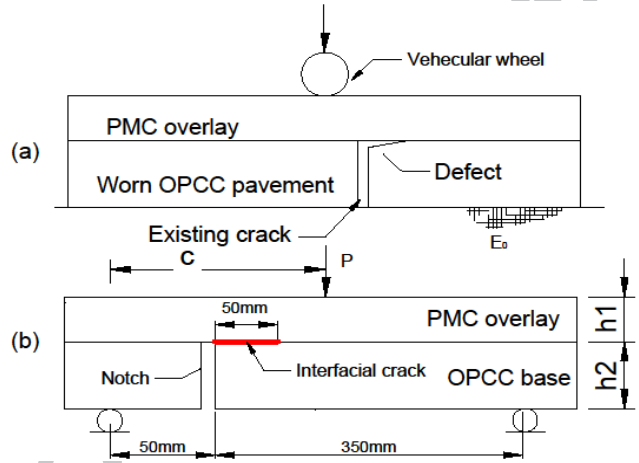

Figure 3. (a): Vehicular wheel-load acting on overlay pavement system with a defect at interface and; (b): Corresponding laboratory configuration of (a).

During an interfacial fracture, the crack propagating along the interface is usually constrained within the interface due to the fact that the bond strength is, normally, lower than that of the top and bottom materials. Earlier studies by the authors [31] suggest that for an actual (typical) overlay pavement system on elastic foundation subjected to vehicular loads, the interfacial crack suffers chiefly from mode-I (opening) damage. The ERR for mode-II (sliding) is only about 3%–12% of the ERR for mode-I, while the ERR for mode-III (tearing) is virtually non-existing. Compared to the double fracture parameters (ERR and phase-angle), a single

fracture parameter, the energy release rate (ERR), is much more convenient to handle in engineering applications. Hence, efforts will be focused on obtaining the interfacial fracture toughness.

4. Measurement of Interfacial Fracture Toughness

4.1 Specimen preparation

The composite beams used for the 3PB test, had a 50mm long interfacial notch created by sticking a heavy-duty masking tape on the OPCC base prior to casting the polymer-modified concrete (PMC) mix (Figure 6(a)). The width of the crack was therefore 0.3mm, equal to the thickness of the tape used. A vertical notch was saw-cut through the OPCC base, 50 mm to the right of the left support. Two groups of composite beams were prepared: One was made with a rough interface on the OPCC side, and the other with a smooth interface, as shown in Figure 4.

The span and width of all beams were kept constant at 400 and 100 mm respectively. The heights of the PMC overlay and OPCC base are reported in Table 2. Distances between the loading point and the left support were 150 mm and 200 mm for the rough and smooth interface composite beams to obtain interfacial debonding for both types of specimens.

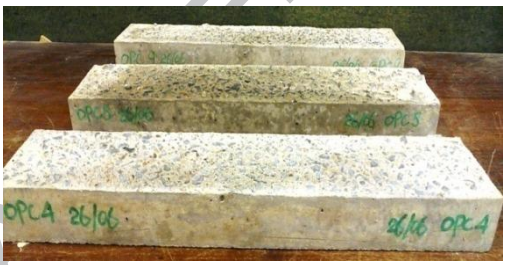

(a)

Figure 4 (a): OPCC bases with rough interfaces; (b): OPCC bases with smooth interfaces

The bi-material beams, for measuring the interfacial fracture toughness, consisted of steel fibre-reinforced, roller-compacted, styrene butadiene rubber (SBR) polymer modified concrete overlay and OPCC base. The overlay mix ID was SBRPMC1.5%-35 (percentage denotes quantity of steel fibres in volume, and steel fibre length of 35mm). Mix proportions and

mechanical properties of the two mixes are listed in Table 1. The methods for testing and assessing their mechanical properties, complyed with British Standards, and are described in refs. [27, 31]. The PMC overlay was formed using a vibrating compactor, whereas the conventional OPCC was consolidated on the vibrating table. At first, the OPCC base was cured in air for 24 hours. Then the whole composite beams with PMC overlay were de-moulded and cured in water for five days, followed by air curing until the test day. Details about the ingredient materials, specimen formation method, curing procedures, etc., can be found in refs. [27,28,29].

Table 1. Mix proportion and mechanical properties of mixes SBRPMC1.5% and OPCC.
(C= cement, CA= coarse aggregate, f_c= comp strength, f_p= max. flexural strength under 3PB, μ =Poison's ratio)

Mix ID	Mix Proportion						Mechanical Properties			
	C	CA	Sand	SBR	Added water	Fibre by vol.	f_c (MPa)	f_n(MOR) (MPa)	E (MPa)	μ
SBRPMC1.5%	1	1.266	1.266	0.217	0.095	1.50%	79.6	15.22	32365	0.187
OPCC	1	2.776	1.612	0	0.506	0%	60.4	4.66	25200	0.21

All OPCC bases were at least 14 days old prior to casting the PMC overlay. The average texture depth of roughened OPCC surfaces was 1.65mm, measured by the sand patch method [27, 33]. No interfacial notch was introduced to the composite beams for the shear tests (Figures 5(b) & 6(b)), except for the OPCC bases that were centrally saw-cut up to the interface as shear tests were aimed at measuring the shear strength of PMC alone. This constituted a parallel research by a colleague.

Table 2. Description of composite beams used for measurement of interfacial fracture toughness. For values of c refer to Figure 7(a).

Beam ID	No. of Beams	Mix ID PMC overlay	OPCC interface	Dimensions WxHxL (mm)	Load. mode
SBRPMC1.5% -on-OPCC-R	3	SBRPMC1.5%	Rough	PMC overlay: 100x72x500	3PB c=150 mm
SBRPMC1.5% -on-OPCC-S	3	SBRPMC1.5%	Smooth	OPCC base: 100x48x500	3PB c=200 mm
SBRPMC1.5% -on-OPCC-R	2	SBRPMC1.5%	Rough		Shear Load

4.2 Experimental set-up and tests procedures

Figures 5 (a) & (b) show the experimental setup of composite beams with a horizontal interfacial notch under three-point bending (3PB) test. The loading rate of 3PB test was controlled by the clip gauge mounted at the mouth of the horizontal interfacial notch. The following loading procedure was applied: The loading rate was kept to 0.0001mm/s until the crack mouth opening displacement (CMOD) reached 0.2mm. Then it was increased to 0.0002mm/s until the CMOD reached 0.5mm; 0.001mm/s until the CMOD was equal to 2mm; finally, 0.003mm/s to beam failure. Very low loading rates ae in general associated a very low crack extension along the interface. Thus the load reading and cracking length were easily recorded manually with the aid of a spotlight and a powerful magnifying glass.

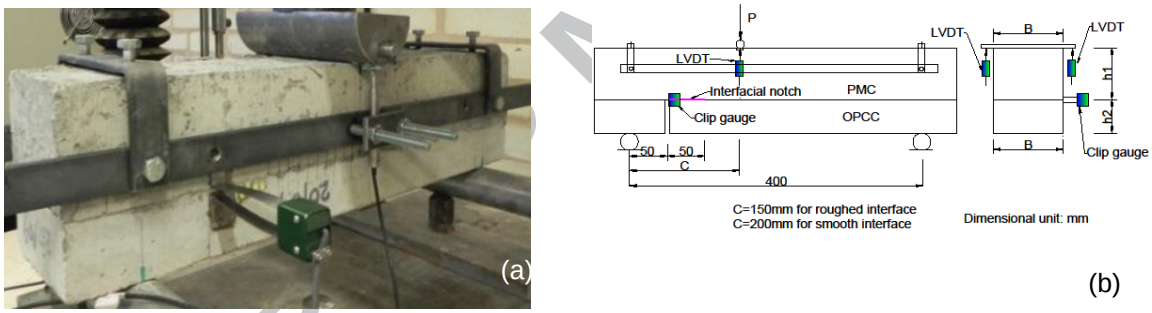

Figure 5. PMC-on-OPCC composite beam with interfacial notch, under 3PB test. (a): Laboratory arrangement. (b): Diagrammatic representation.

Figures 6 (a) & (b) show the experimental setup of composite beams with a vertical notch through the OPCC base, undergoing tests to measure the shear strength of PMC overlay. Unfortunately, one of the three composite beams exhibited partial interfacial delamination before the cracks finally penetrate vertically into the PMC layer. This is attributed to a small segment (23mm-long) of the beams being predominantly under bending, resulting in delamination at the interface. The loading rate was slow, 0.00001 mm/s, controlled by the vertical displacement, measured at the position of the top roller

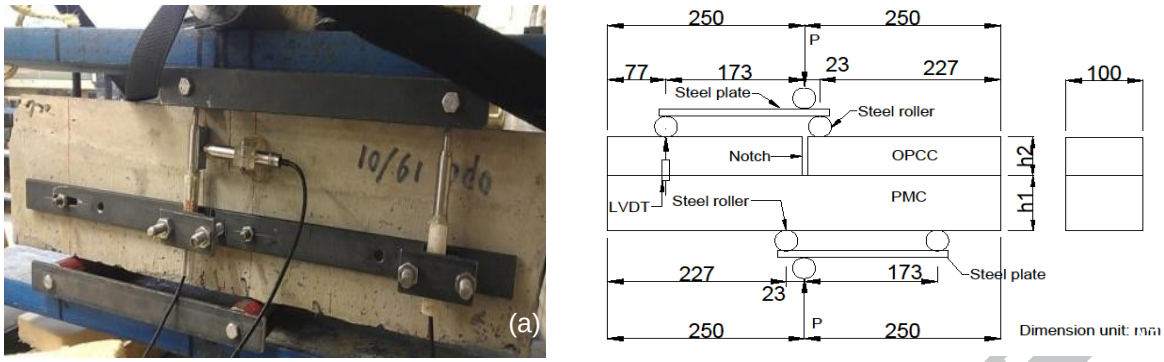

Figure 6. PMC-on-OPCC composite beam with notch through OPCC base under shear test. (a): Laboratory arrangement. (b): Diagrammatic representation.

4.3 Experimental results

As the crack extended and propagated very slowly along the interface, the stress field ahead of the crack tip was always at a critical state (about to cause the crack to extend), implying that the ERR was also at a critical state, and therefore equal to interfacial fracture toughness.

Careful observation during testing, that is, searching for cracks using an illuminated, high power magnifying glass, at the front and rear of the specimens, suggested that all eight composite beams suffered interfacial delamination. It was reasoned that if the crack appeared symmetrical on both sides of the specimens, that would provide further assurance of its real trajectory. Finally, as an additional check, every specimen (there were hundreds of them tested during the research) was taken down the test-rig and its failure mode was meticulously inspected to verify that the observed surface failure occurred also inside the material. The above provided additional confidence for the data collected.

Figure 7 illustrates typical crack trajectories in the beams. Typical interfacial delamination is shown in Figure 8. The results were taken from a research (doctoral) study [27] and shown in Table 3. It is pointed out that, for the composite beams exhibiting a crack trajectory shown in Figure 7(b), the load recorded in Table 3 corresponds to the crack propagating along the path 1-2 (interfacial cracking), as opposed to 3-4-5, to obtain a simple mechanical model and accurate interfacial fracture toughness.

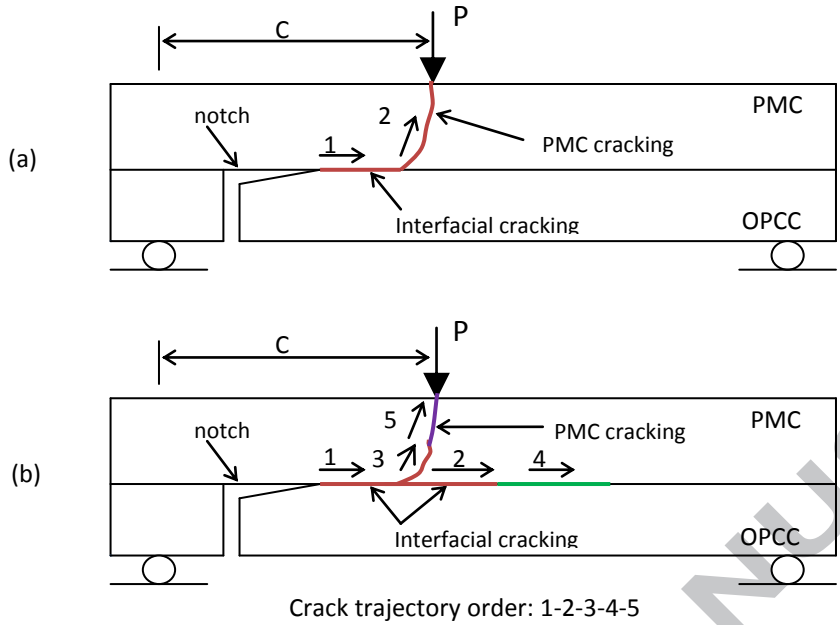

Figure 7. Crack trajectories. (a): Type-1. Crack initiated at notch tip, extended along the interface and finally penetrated obliquely the PMC; (b): Type-2. Crack initiated at notch tip (1→), it extended into the interface (2→), penetrated obliquely the PMC (3→), propagated along the interface again (4→), and finally appeared at the top under the loading position (5→).

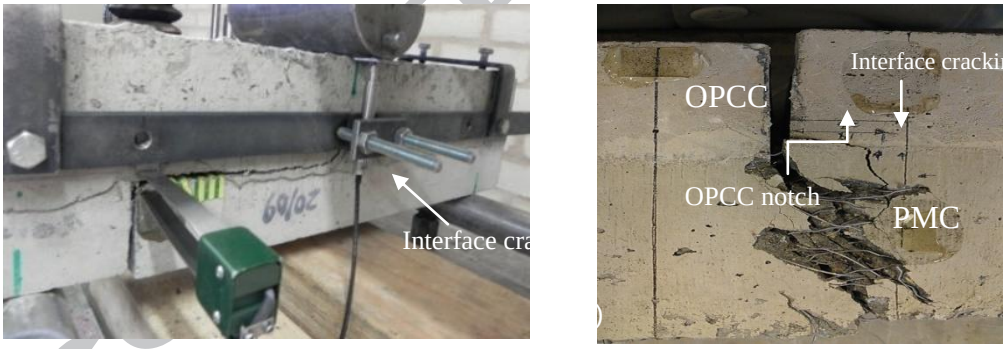

Figure 8. Interfacial debonding of composite beams. (a): 3PB test, (b): Shear test. Note that (b) is shown upside down for clarity.

The critical ERRs at interface (interfacial fracture toughness, G_{ic}, shown in Table 3) were calculated using the method proposed in Section 2 of this article. Load readings and corresponding crack lengths were recorded in the laboratory.

4.4 A numerical analysis approach.

The FE code ANSYS10.0 [30] was employed since the analytical solution for the mechanical models illustrated in Figures 5 and 6 is unavailable. The area around the crack tip was fine-meshed with square elements of edge length 0.1 mm. The ratio of element size to crack length was kept below 0.01. The constant strain, PLANE42 element was chosen for the fine-meshed zone. This element is defined by four nodes having two translational degrees of freedom (DOF) per node. It has a number of simulation capabilities allowing for plasticity, stress stiffening, large deflection and strain. The non-linear solution output is in nodal displacements per integration point. It is therefore recommended for micro-mechanics, that is, detailed modelling cracked regions and slow crack propagation. In addition, the SPRING14 element offering longitudinal uniaxial tension-compression with up to three degrees of freedom at each node was used to connect the three nodes at the crack tip and allow for stiffness reduction (Figure 2(c)). Plane strain conditions were assumed throughout. The number of nodes for a typical model was approximately 30,000. The crack extension for all models was Δa= 0.1 mm. The predicted deformed shape is shown in Figure 9 and the interfacial fracture toughness, G_{ic}, results are listed in Table 3.

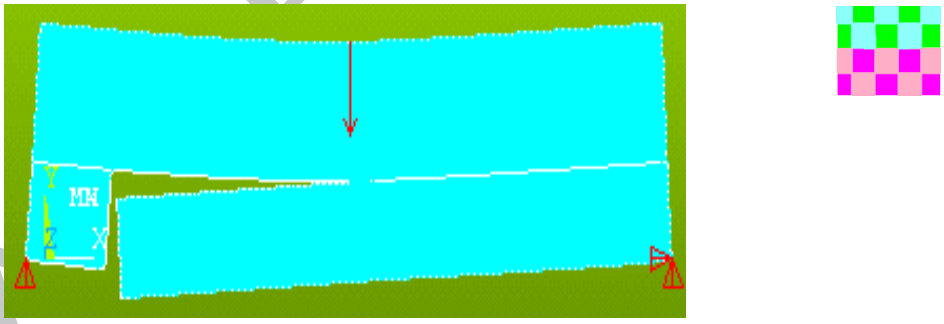

Figure 9. Deformed composite beam undergoing 3PB test simulated in ANSYS FE code; Inset: Square elements in fine meshed, cracked zone.

Table 3. Displays dimensions of composite beams, experimental load results and corresponding crack lengths. The calculated interfacial fracture toughness of SBRPMC1.5%-on-OPCC composite beams is also listed

Interface condition	Loading mode	Dimension of beams			Lab Results		Calculated Results		
		h_1	h_2	a_0	p	a	G_{ic}	ψ_G	Average G_{iC}
		mm	mm	mm	N/mm	mm	J/m^2	Deg.	J/m^2
Rough	3PB	71	47	50	132	56	46.2	11.86	52
interface	test	70	47	50	131	87	64.0	33.67	
		68	48	50	124	50	51.3	17.2	
				50	109	80	64.6	19.68	
Rough	Shear	49	71	0	569	18	51.9	16.99	
interface	test	50	74	0	545	12	46.0	3.06	
				0	575	19	40.1	8.27	
Smooth	3PB	70	50	50	100	155	28.6	30.19	22.6
interface	test	72	48	50	108	200	10.3	79.01	
		71	50	50	110	70	28.9	10.80	

Note: Load p, is listed for 1 mm width beam, not the total load.

Table 3 shows that the interfacial fracture toughness (G_{ic}) of theSBRPMC1.5%-on-OPCC composite beam with rough and smooth interfaces is 52 J/m^2 and 22.6 J/m^2, respectively; the former is approximately 2.3 times the latter. Also, Table 3 shows that ψ_G, the phase-angle, characterising the ratio of $ERR_{(sliding)}/ERR_{(opening)}$, is in the range of: $3.06^0 \leq \psi_G \leq 33.67^0$. These values of ψ_G enclose those at the interface of an actual overlay pavement subjected to typical 2x120 kN and 190 kN vehicular axle loads, which are 3° and 7° respectively and are reported in Table 9, reference [31], by the authors. This can only imply that the measured interfacial fracture toughness listed in Table 3 can be suitable for concrete overlay pavement design.

Figure 10 demonstrates the relationship between G_{ic} and $tan\psi_G$ for both rough and smooth interfaced beams. It is seen that the interfacial fracture toughness, G_{ic}, appears to be insensitive to the variation of $tan\psi_G$ for these composite beams. This implies that a single fracture parameter, G_i, is sufficient to characterise the behaviour of interfacial fracture for the mechanical models shown in Figures 5, 6 and 7, at least for engineering applications.

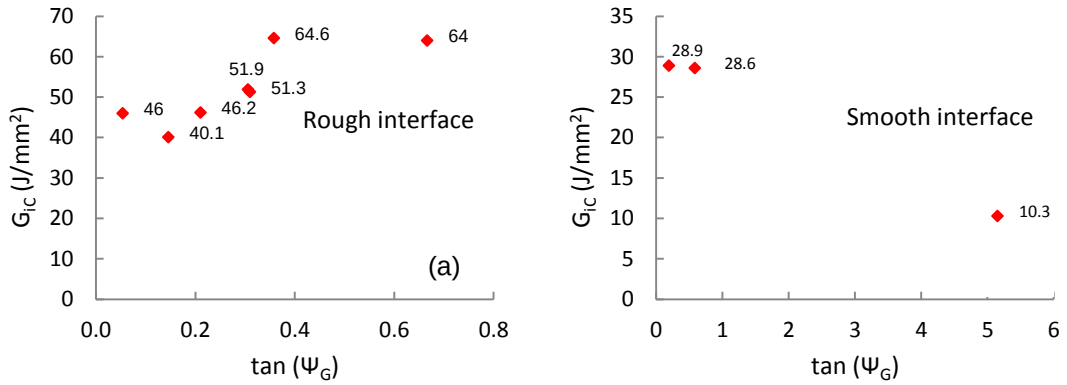

Figure 10. Relationship between interfacial toughness, G_{ic}, and phase angle, $tan\psi_G$, for SBRPMC1.5%-on-OPCC composite beams. (a): beams with rough interface; (b): beams with smooth interface.

4.5 Splitting tensile bond strength

After the 3PB test above, the same PMC-on-OPCC composite beams were saw-cut to prisms to obtain the splitting tensile bond strength (Figure 11). The test procedure complied with BS EN 12390-6:2009 [34]. The loading rate was 1.4 kN/s. The splitting tensile bond strengths can be found in Table 4. It is obvious that the strength of prisms SBRPMC1.5%-on-OPCC-R (rough interface) is much higher than that of SBRPMC1.5%-on-OPCC-S (smooth interface).

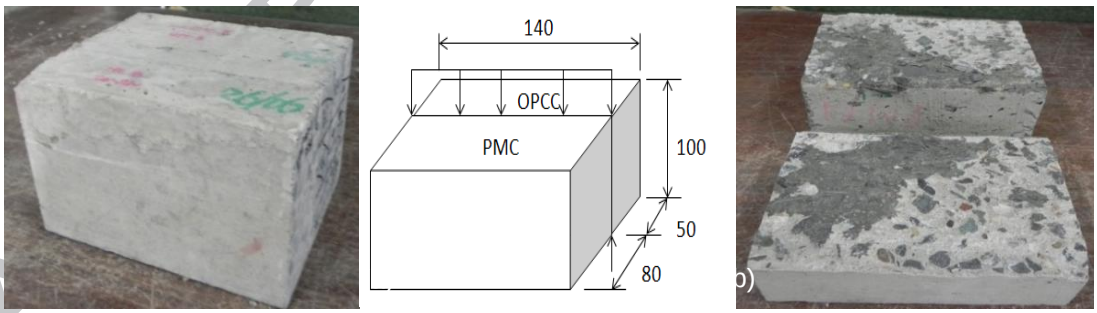

Figure 11. (a): Typical prism sawn-cut from a used composite beam; (b): Typical dimensions; (c): A PMC patch is left bonded on OPCC interface after the splitting test.

Table 4 Splitting tensile bond strength of prisms sawn-cut from tested SFRPMC-on-OPCC composite beams

ID of composite beams	OPCC interface	Number of specimens	Average (MPa)	STDEV (MPa)
SBRPMC1.5%-on-OPCC	Rough	10	2.96	0.47
SBRPMC1.5%-on-OPCC	Smooth	6	1.80	0.19
OPCC-on-OPCC	Rough	7	2.68	0.28

The splitting tensile bond strengths, measured from sawn-cuts of the tested composite beams were 2.96 MPa for the rough and 1.80 MPa for the smooth interface beams. The former is 1.64 times the latter.

5. Interfacial Behaviour of a Composite Beam under 4PB. – Validation

Four point bending (4BP) tests were conducted by the authors on SFRPMC-on-OPCC composite beams to explore their flexural performance [27]. In order to gain more confidence in the procedure of ERR calculation, and to explore the interfacial delamination behaviour further, two of the tested composite beams were analysed utilising the 4PB test and fracture mechanics at the interface. The results were compared with the experimental results.

In the SFRPMC-on-OPCC composite beam, cracking initiates from the bottom of the OPCC base. When the crack reaches the interface, it will either penetrate into the top layer without debonding (good quality bond), or it will deflect into the interface (poor quality bond). He and Hutchinson [35] proposed a "*competition criterion"* for a crack impinging the interface, demonstrated in Figure 12. The impinging crack is likely to be deflected into the interface if inequality (5) is satisfied. Conversely, the crack will tend to penetrate the interface when inequality (5) is reversed:

$$\text{If: } \frac{G_{ic}}{G_c} \leq \frac{G_d}{G_p} \quad \text{Then: Crack deflects into interface} \tag{5}$$

$$\text{If: } \frac{G_{ic}}{G_c} \geq \frac{G_d}{G_p} \quad \text{Then: Crack penetrates PMC} \tag{6}$$

where: G_{ic} and G_c are the fracture toughness (critical ERR) of the interface and the toughness of the top layer material in mode-I loading. G_d and G_p are the (strained) ERRs needed for deflection into the interface, and penetration into the top material, respectively.

Both G_d and G_p are computed by assuming crack extension of a small amount, Δa. For the computation of G_p, the crack tip is in the top layer, and thus the stress field at the crack tip is dominated by the homogeneous material.

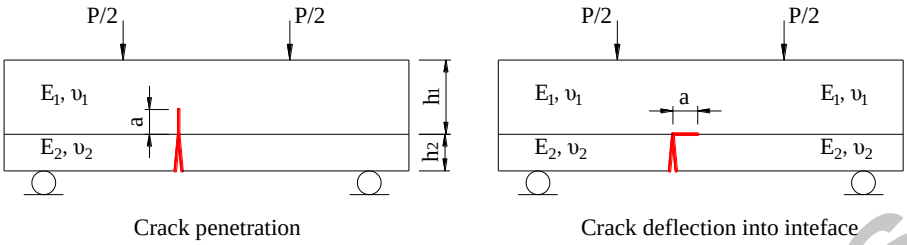

Figure12. "*Race*" for crack penetration into the top layer, or deflection into the interface under 4PB tests.

For a crack in a single material, crack fracture is traditionally characterized by the stress intensity factors (SIF), K_I and K_{II}, instead of the energy release rate, although both can be correlated. For a crack in a homogeneous material under mixed mode loading, Broek [36] proposed a general criterion for crack extension given by:

$$\left(\frac{K_I}{K_{IC}}\right)^{\alpha} + \left(\frac{K_{II}}{K_{IIC}}\right)^{\beta} = 1 \tag{7}$$

where: K_I, K_{II}, K_{IC}, K_{IIC} are SIFs and critical SIFs for mode-I and mode-II loadings, respectively; α and β are material constants.

In the present composite beam under 4PB, K_{II} is comparatively small and can be ignored. Thus, a simple criterion for vertical penetration into the top material is given by:

$$K_I \geq K_{IC,M}^{ini.} \tag{8}$$

where: $K_{IC,M}^{ini.}$ is the critical SIF at crack initiation at the tip of the notch, in mode-I loading.

It is stressed that $K_{IC,M}^{ini.}$ is the critical SIF of the matrix (mix without fibres) as the fibres in the matrix are inactive before cracking. The $K_{IC,M}^{ini.}$ of matrix SBRPMC0% is 24.63 MPa·mm$^{0.5}$,

which can be found in Table 3, Reference [37] by the authors. The matrix relates to mix SBRPMC1.5%-35.

For crack deflection and propagation in the interface, the single mechanical parameter, i.e. strain energy release rate, G_i, may characterize suitably the interfacial delamination behaviour, because the interfacial bond strength is usually much weaker than the strength of both materials, and thus the crack propagation is constrained within the interface. Based on this argument, the single parameter, G_i, is used to assess crack propagation at interface; namely the crack is likely to deflect and/or extend in the interface if the following inequality is satisfied:

$$G_i \geq G_{ic} \tag{9}$$

where: G_i is the ERR at the interface, and G_{ic} is the interfacial fracture toughness (namely the critical interfacial ERR).

5.1 Interfacial behaviour of a composite beam – Rough interface

The composite beam SBRPMC1.5%-on-OPCC with rough interface shown in Figure 13, fractured vertically, without interfacial delamination, under a 4PB test [27]. The rate of loading was 0.0001mm/s, controlled by the mid-span vertical displacement. The ingredients of SBRPMC1.5% and OPCC, the specimen formation method and the curing procedure were as described earlier. The crack initiated at the bottom of the OPPC base, 140 mm away from the left support, and gradually penetrated the PMC layer to failure, without the presence of interfacial debonding.

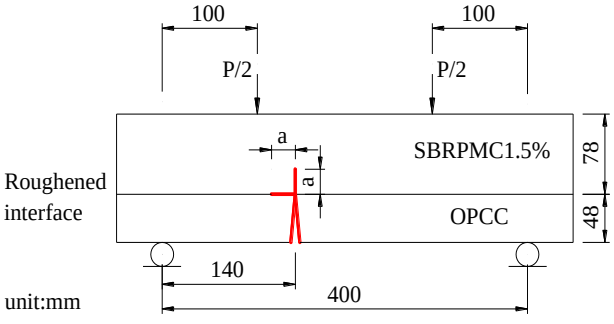

Figure 13. (a): SBRPMC1.5% overlay-on-OPCC base composite beam, under 4PB test. (b): Dimensions and cracking configuration of the beam.

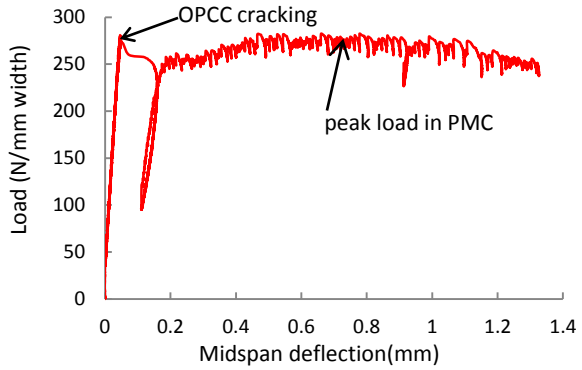

Figure14. Experimental load vs. mid-span deflection of the beam in Figure 13.

The fracture behaviour of the composite beam, when a crack reaches the interface is considered by comparing the calculated K_I and G_i with the criteria proposed earlier (inequality 9). From Figure14 it can be seen that OPCC started cracking at 281 N/mm width, then the load dropped to 102 N/mm width in a displacement-controlled loading mode. Therefore, the load p, corresponding to crack impinging the interface, should lie within the range: $102 \leq p \leq 281$ N/mm width.

Considering the lower (conservative) case of p= 102 N/mm width of beam, and referring to Figure 13(b), for a crack impinging the interface, both, K_I for vertical penetration, and G_i for deflection to the left interface, were calculated for crack lengths of 2, 5 and 10 mm, and listed in Table 5. The crack length chosen is mainly dependent on the maximum size of coarse aggregate; in this case 10 mm for both mixes SBRPMC1.5%-35 and OPCC. A possible defect may thus be in the range of 0 – 10 mm. The calculation procedure for G_i has been presented earlier.

Table 5. SIF-K_I for penetration into the top layer, and ERR-G_i for deviation into left interface of SBRPMC1.5%-on-OPCC beam with rough interface under 4PB test.

Crack Length a (mm)	Penetration into Top Material K_I(MPa·mm$^{0.5}$)	Deflection into Interface G_i(Jm^{-2})
2	29.6	5.0
5	30.8	4.4
10	34.8	4.0

It is seen from Table 5 that all K_I – Penetration into Top Material, exceeded the critical value of $K_{IC,M}^{ini.} = 24.63$ MPa·mm$^{0.5}$, that is, the critical crack initiation SIF of matrix SBRPMC0%. In contrast, all calculated values of interfacial ERRs G_i – Deflection into Interface, are much lower than the corresponding measured interfacial fracture toughness value of 52 J/m^2 (Table 3). This predicts that the beam fails by fracturing (cracking) through the top layer without any interfacial delamination present. Therefore, the predicted (analytical) values are in agreement with the experimental results.

5.2 Interfacial behaviour of a composite beam – Smooth interface

The composite Beam-6 in Table 7-3 of reference [27] by the authors is considered. This consisted of SBRPMC1.5% overlay and OPCC base with smooth interface. The crack trajectory is visible in Figure15 (a) & (b). This Figure discloses that after reaching the interface, the crack swerved towards the right, propagating into the interface for approx. 33 mm. It was observed that the left interface debonded immediately after that. The crack trajectory followed the path 1-2-3-4-5. The corresponding load reading when the crack reached the interface was 244 N/mm width of beam.

The two models shown in Figure16 were studied. For Model-1, showing the crack impinging the interface, penetration into top layer and deviation into the interface were considered. For Model-2, the G_i at points A (crack just reached interface) and B (crack propagated through interface) were investigated while the crack moves from A-to-B-to-C.

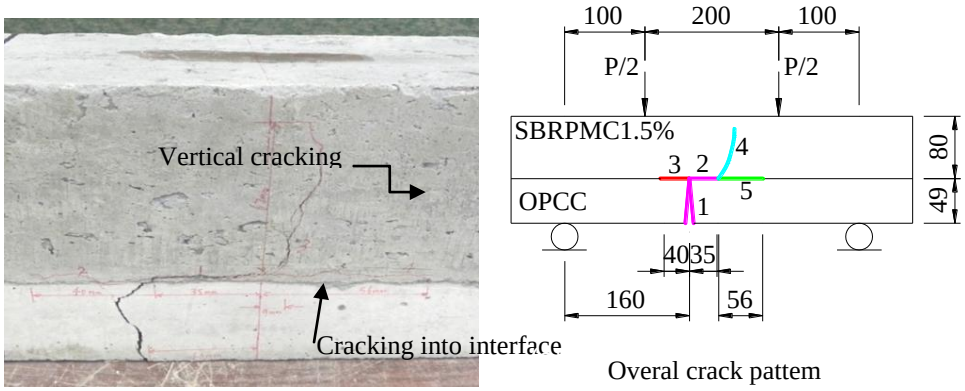

Figure 15. (a): Actual cracking pattern of composite Beam-6 under 4PB test. (b): Crack propagation into interface due to poor bond, and crack extension trajectories: 1-2-3-4-5.

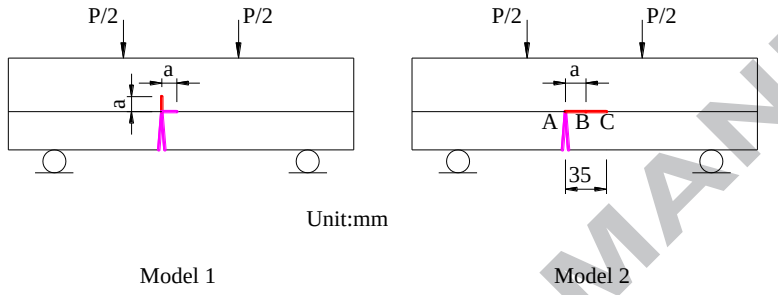

Figure16. Two cracked models of composite Beam-6 with smooth interface, under examination. Model-1: penetration into top layer, or deflection into interface as crack impinging interface. Model-2: Crack propagating along the right interface.

Model-1

In Model-1, the K_I-penetration and G_i-deflection were calculated using the method presented earlier. The calculated results with crack lengths of 2, 5 and 10 mm are presented in Table 6. It can be seen that both K_I and G_i exceeded their critical values of 24.63 MPa·mm$^{0.5}$and 22.6 J/m^2 respectively under the load of 244 N/mm width. The experimental result indicated that the crack deflected into the right interface and propagated 33 mm along the latter. This might be attributed to the unevenness of bond quality (difference between concrete paste and aggregate consisting the interface).

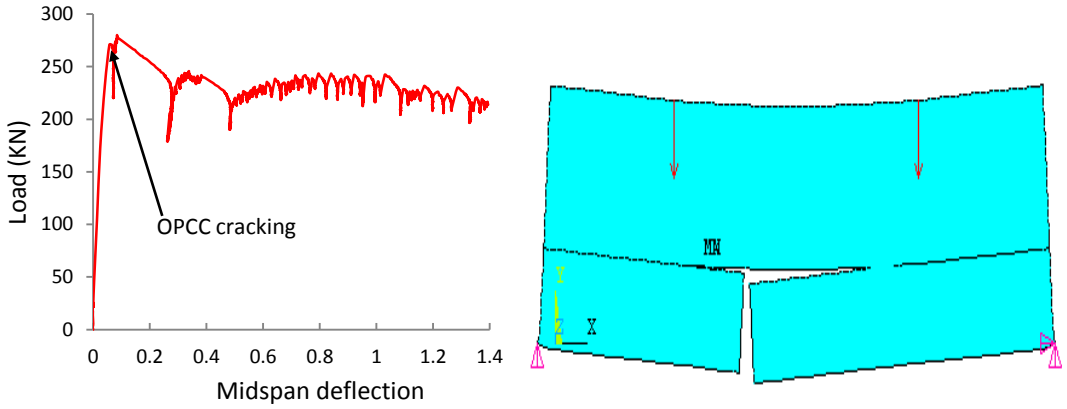

(a) (b)

Figure17. (a): Experimental load-midspan deflection of composite beam with smooth interface. (b): Simulation of loaded composite beam with interfacial debonding.

Table 6. Crack impinging the interface: K_I-penetration into top layer, or G_i-deflection into right interface of Model-1 in Figure 17 (load p= 244N/mm width of beam)

Crack Length a (mm)	Penetration into top Material K_I (MPamm$^{0.5}$)	Deflection into Interface G_i (J/m^2)
2	66.8	25.9
5	72.6	26.2
10	81.1	25.7

Model-2

In Model-2, Figure 16, and after the crack has propagated along the right interface, if and when (at what stage) it swerves into the left interface, depends on the values of G_{iA} and G_{iB}, since the interfacial fracture toughness is even along the interface. The calculated values of G_i at points A and B as the crack propagated into the right interface are listed in Table 7 in a *ratio form*, since G_i is linearly proportional to the load P in theory of elasticity.

Table 7. ERR-ratios at points A and B during the process of crack propagation to the right interface, from point A to B to C (Model 2, Figure 16).

a (mm)	0	2	5	10	20	35
G_{iA} (normalised)	1	1.01	1.02	1.05	1.10	1.13
G_{iB} (normalised)	_	1.01	1.02	1.05	1.09	1.1

The first row (a-mm), displays values of crack position (extension) along the interface (0, 2, 5, 10, 20, 35) in mm. The second row (G_{iA}), provides ERR ratios (eg: G_{iA} at position 2, divided by G_{iA} at position 0, and so on, that is, values of G_{iA} normalised to position 0) for crack extensions along the right interface. Similarly, the third row (G_{iB}), provides ERR ratios for crack extensions along the left interface.

To understand Table 7, let us take the case of a= 35mm. In this case model 2, Figure 17(b), with the right interfacial crack of 35mm will be used to calculate the G_i at points A and B. Referring to Figure 17(a), model 2, with the crack impinging the interface, a=0mm. In this case one can compute the ERR, that is $G_{iA(\,a=0)}$, at point A, by assuming the crack extends into the left interface by a small amount, Δa= 0.1mm.

Now consider Figure 17(b), model 2, with the crack having travelled into the right interface, a= 35mm. In this case one can compute the ERRs, that is $G_{iA(\,a=35)}$, and $G_{iB(\,a=35)}$, respectively. One can now obtain the ratio of: $G_{iA(a=35)}/G_{iA(a=0)} = G_{iA}$. And as $G_{iA(a=0)} = G_{iB(a=0)}$, the ratio $G_{iB(a=35)}/G_{iA(a=0)} = G_{iB}$.

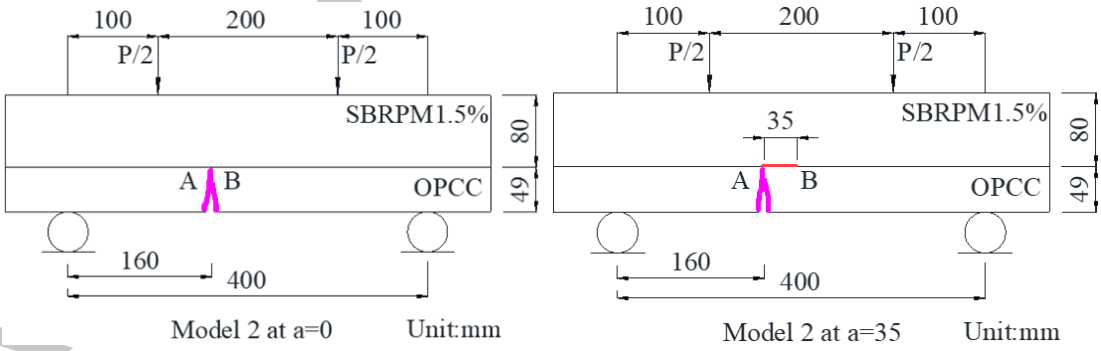

Figure 17 Model-2, at a= 0mm and a= 35mm

It is seen from Table 7 that the ERR at both points A and B increased during crack propagation along the right interface from point A-to-B and beyond to C (Figure 16) but the incremental rate of the former, G_{iA}, was slightly higher than that of the latter G_{iB}. In fact, G_i at A was larger than G_i at B, for crack lengths larger than 20 mm.

Consequently, the analytical approach above, predicts that after the crack has moved 20 mm towards the right interface, the left interface starts debonding from point A. This prediction is fundamentally in agreement with the experimental results. The corresponding experimental results showed that the left interface started debonding at point A, when the crack had already propagated 33 mm to the right interface. The minor discrepancy between 20mm and 33mm can be attributed to the variation of bond quality in the laboratory (the presence of a coarse aggregate).

Summarising the analysis above, the single parameter G_i is capable to suitably characterize the crack propagation into the interface, while the method proposed earlier to calculate the G_i is an appropriate method.

6. Concluding Remarks

A simple numerical approach for the determination of the interfacial energy release rate, based on the theory of elasticity and using crack closure and the nodal force technique, has been proposed. It was assisted by finite element analysis and experimentation and verified by comparing the calculated results with experimental data available. It is hoped that the simplicity of the method will be useful to practicing engineers.

A test model for measuring the interfacial fracture toughness of a bi-material interface for concrete overlaid pavements was developed. The measured interfacial fracture toughness of steel fibre-reinforced, roller-compacted, polymer modified concrete to ordinary Portland cement concrete was found to be 52.0 J/m^2 and 22.6 J/m^2 for rough and smooth interfaces, respectively. Validation showed that the analytical prediction is in line with the experimental results.

Essentially, it was emphasised that composite beams will fail by fracturing (cracking) through the top layer, without suffering any interfacial delamination through their roughened interface. It was also shown that the prediction based in Model 2 is fundamentally in agreement with the experimental results.

The experimental setup and the measured interfacial fracture toughness can be utilised for the design of overlay on worn concrete pavements.

It was found that the single interfacial fracture parameter, the ERR (energy release rate) at interface, is an appropriate, sufficient and reliable parameter to assess the interfacial delamination performance of a composite beam under flexure.

Acknowledgments:

The financial support of the Engineering and Physical Sciences Research Council (EPSRC Ind. Case Studentship No. 08002550), and Aggregate Industries, UK, is gratefully acknowledged. The authors would like to express their gratitude to their colleague, Dr. Yi Xu, for her valuable help during the laboratory work. Tarmac should also be mentioned for providing materials for research.

References

[1] Delatte, N.J. (1998). Investigating performance of bonded concrete overlays, *Journal of performance of constructed facilities*, May 1998, pp.62-70.

[2] Delatte, N. J., Sehdev, A. (2003). Mechanical properties and durability of bonded-concrete overlays and ultrathin white-topping concrete, *Journal of Transportation Engineering*, 2003, pp.16-23.

[3] NCPTC (National Concrete Pavement Technology Centre), USA; (2008). Guide to concrete overlays (second edition), September. 2008.

[4] Soares, J.B., Tang, T. (1998). Bi-material Brazilian specimen for determining interfacial fracture toughness, Engineering Fracture Mechanics, 1998, Vol. 59, No. 1, pp. 57-71.

[5] Tong, J., Wong, K.Y., Lupton, C. (2007). Determination of interfacial fracture toughness of bone-cement interface using sandwich Brazilian disks, *Engineering Fracture Mechanics* 74 (2007) 1904–1916

[6] Matos, P.P.L., McMeeking, R.M., Charalamides, P.G., Drory, D. (1989). A method for calculating stress intensities in bi-material fracture, *International Journal of Fracture*, 40, 313-322.

[7] Sun, C.T., Jih, C.J. (1987). On strain energy release rates for interfacial cracks in bi-material media, *Engineering Fracture Mechanics*, Vol. 28, No. 1, pp. 13-30.

[8] Sun, C.T. and Qian, W. (1997). The use of finite extension strain energy release rates in fracture of interfacial cracks, *International Journal of Solids and Structures*, Vol. 34, No. 20, pp. 2595-2609.

[9] Shi, X.Q., Zhang, X.R., Pang, J.H.L. (2006). Determination of interface fracture toughness of adhesive joint subjected to mixed-mode loading using finite element method, *International Journal of Adhesion and Adhesives*, 26 (2006) 249-260.

[10] Bjerkén, C., Persson, C. (2001). A numerical method for calculating stress intensity factors for interface cracks in bi-materials, *Engineering Fracture Mechanics*, 68 (2001) 235-246.

[11] Matsumto, T., Tanaka, M., Obara, R. (2000). Computation of stress intensity factors of

interface cracks based on interaction energy release rates and BEM sensitivity analysis. *Engineering Fracture Mechanics*, 65(6), 683–702.

[12] Xie, D., Biggers Jr., S.B. (2006). Progressive crack growth analysis using interface element based on the virtual crack closure technique, *Finite Elements in Analysis and Design* 42 (2006) 977- 984.

[13] Rybicki, E.F., Kanninen, M.F., (1977). A finite element calculation of stress intensity factors by a modified crack closure integral, *Engineering Fracture Mechanics*, 1977, 9:931-938.

[14] Irwin, G.R., Fracture, Handbuch der Physic. 6, 551 (1958).

[15] Sridharan, S. (2001). Displacement-based mode separation of strain energy release rates for interfacial cracks in bi-material medias, *International Journal of Solids and Structures*, 38(2001) 6787-6803.

[16] Charalambides, P.G.; Lund, J.; Evans, A.G.; McMeeking, R.M.; (1989). A Test Specimen for Determining the Fracture Resistance of Bimaterial Interfaces, Journal of Applied Mechanics, 56(1989), 77-82.

[17] Klingbeil, N.W., Beuth, J.L. (1997). Interfacial fracture testing of deposit metal layers under four-point bending, *Engineering Fracture Mechanics*, Vol. 56, No.1, pp.113-126.

[18] Huang, Z., Suo, Z., Xu, G., He, J., Prevost, J.H., Sukumar, N. (2005). Initiation and arrest of an interfacial crack in a four-point bend test, *Engineering Fracture Mechanics* 72 (2005) 2584–2601.

[19] Watanabe, T. (2009). Interfacial fracture mechanics approach to delamination resistance between cement-based materials, *Journal of Engineering Mechanics*, Vol. 135, No.10, pp.1198-1205.

[20] Wang, J.-S.; Suo, Z.; 1990, Experimental determination of interfacial toughness curves using Brazil-nut-sandwiches, *Acta, metal, materials*, Vol. 38, No. 7, pp. 1279 – 1290.

[21] Shi, X.Q., Zhang, X.R., Pang, J.H.L. (2006). Determination of interface fracture toughness of adhesive joint subjected to mixed-mode loading using finite element method, *International Journal of Adhesion and Adhesives*, 26 (2006) 249-260.

[22] Büyüköztürk, O., Lee, K.M. (1993). Assessment of interfacial fracture toughness in concrete composite, *Cement and Concrete Composite*, 15 (1993) 143-151.

[23] Tschegg, E.K., Tan, D.M., Kircher, H.O.K, Stanzl, S.E. (1993). Interfacial and sub-interfacial fracture in concrete, *Acta, Metallurgica et Materialia*, Vol.41, No.2, pp.569-576.

[24] Satoh, A., Yamada, K., Ishiyama, S. (2010). A discussion on major factors affecting crack path of concrete-to-concrete interfacial surfaces, *Engineering Fracture Mechanics* 77 (2010) 2168 – 2181.

[25] Chabot, A., Hun, M., Hammoum, F. (2013). Mechanical analysis of a mixed mode debonding test for 'composite' pavements, Construction and Building Materials 40 (2013) 1076 – 1087.

[26] Chabot, A., Hammoum, F., Hun, M. (2017). A 4pt Bending Bond Test Approach to Evaluate Water Effect in a Composite Beam, European Journal of Environmental and Civil Engineering, Taylor & Francis, 2017.

[27] Lin, Y. (2014). Optimum Design for Sustainable 'Green' Bonded Concrete Overlays: Controlling Flexural Failure, Doctoral Thesis (PhD), Coventry University, UK (unpublished).

[28] Lin, Y., Karadelis, J.N., Xu, Y. (2013). A new mix design method for steel fibre-reinforced,

roller compacted and polymer modified bonded concrete overlays，*Construction and Building Materials*, 48 (2013) 333－341.

[29] Karadelis, J.N., Lin, Y. (2015). Flexural strengths and fibre efficiency of steel-fibre-reinforced, roller-compacted, polymer modified concrete，*Construction and Building Materials*, 93 (2015) 498－505.

[30] ANSYS, Inc. Southpointe, 275 Technology Drive, Canonsburg, PA 15317, USA. www.ansys.com.

[31] Karadelis, J.N., Lin, Y. (2016). Strain energy release rate at interface of concrete overlaid pavements, *International Journal of Pavement Engineering*, 1029-8436 (Print) 1477-268X (Online).

[32] Poshtan, E.A., Rzepka, S., Michel, B., Silber, C., Wunderle, B. (2014). An accelerated method for characterization of bi-material interfaces in microelectronic packages under cyclic loading conditions, 2014, 15th International Conference on Thermal. Mechanical and Multi-Physics Simulation and Experiments in Microelectronics and Microsystems. EuroSimE 2014.

[33] British Standard, BS 598-105:1990. Sampling and examination of bituminous mixtures for roads and other pavement areas- part 105: Methods of tests for determination of texture depth, UK.

[34] British Standard BS EN 12390-6:2009. Testing hardened concrete Part 6: Tensile splitting strength of test specimens, British Standard Institute, UK.

[35] He, M-Y., Hutchinson J.W. (1989). Crack Deflection at an Interface between Dissimilar Elastic Materials. *Int. Journal of Solids and Structures*, 25, 9, 1053-1067.

[36] Broek, D. (1986). Elementary Engineering Fracture Mechanics, 4th rev.ed., Martinus Nijhoff, Dordrecht, The Netherlands, 1986.

[37] Lin, Y., Karadelis, J.N. (2015). Establishing the fibre bridging law by an inverse analysis approach, *Journal of Materials in Civil Engineering*, ASCE, ISSN 0899-1561/04015105(11).

HIGHLIGHTS

- Model was developed for interface fracture toughness of concrete overlaid pavements
- Interfacial energy release rate determined by crack closure & nodal force technique
- Composite beams will fail by fracturing of top layer; no interfacial delamination
- Measured interfacial fracture toughness can become design guideline for overlays
- ERR at interface, is sufficient, reliable to assess delamination in composite beams